Prediction of Neoadjuvant Chemoradiotherapy Sensitivity in Patients With Esophageal Squamous Cell Carcinoma Using CT-Based Radiomics Combined With Clinical Features

Xindi Li[1,2,]* ⬦, Jigang Dong[1,3,]*, Baosheng Li[4] ⬦, Ouyang Aimei[5], Yahong Sun[2], Xia Wu[2], Wenjuan Liu[6], Ruobing Li[5], Zhongyuan Li[7], and Yu Yang[8]

Abstract

Background: For patients with resectable locally advanced esophageal squamous cell carcinoma (ESCC), the current standard treatment is neoadjuvant chemoradiotherapy (nCRT) plus radical surgery. **Objective:** This study aimed to establish a predictive model, based on computed tomography (CT) radiomics features and clinical parameters, to predict sensitivity to nCRT in patients with ESCC pre-treatment. The goal was to provide risk stratification and decision-making recommendations for clinical treatments and offer more valuable information for developing personalized therapies. **Methods:** This retrospective study involved 102 patients diagnosed with ESCC through biopsy who underwent nCRT. To select radiomics features, we used the least absolute shrinkage and selection operator (LASSO) algorithm. A combined model was constructed, integrating the selected clinically relevant parameters with the Rad-Score. To assess the performance of this combined model, we utilized calibration curves and receiver operating characteristic (ROC) curves. **Results:** Nine optimal radiomics features were selected using the LASSO algorithm. The support vector machine (SVM) classifier was identified as having the best predictive performance. The area under the curve (AUC) of the SVM training group was 0.937 (95% CI: 0.856-1.000), and of the validation group was 0.831 (95% CI: 0.679-0.983). Smoking and alcohol history, neutrophil to lymphocyte ratio, serum aspartate aminotransferase to alanine aminotransferase ratio, and carcinoembryonic antigen and fibrinogen levels were independent predictors of sensitivity to nCRT in patients with ESCC. The AUCs of the combined model for the training and validation groups were 0.870 (95% CI: 0.774-0.964) and 0.821 (95% CI: 0.669-0.972), respectively. The calibration curve showed that the nomogram's predictions were close to the actual clinical observations, indicating that the model

[1] Tianjin Medical University Cancer Institute & Hospital, National Clinical Research Center for Cancer, Tianjin's Clinical Research Center for Cancer, Tianjin Key Laboratory of Digestive Cancer, Tianjin, China
[2] Department of Oncology, Shandong University, Shandong Provincial Third Hospital, Jinan, China
[3] Qingdao Jiaozhou Central Hospital, Qingdao, China
[4] Department of Radiation Oncology, Shandong Cancer Hospital and Institute, Shandong First Medical University and Shandong Academy of Medical Sciences, Jinan, China
[5] Department of Radiology, Central Hospital Affiliated to Shandong First Medical University, Jinan, China
[6] Shandong Provincial Key Laboratory of Radiation Oncology, Cancer Research Center, Shandong Cancer Hospital and Institute, Jinan, China
[7] School of Medical Imaging, Shandong Second Medical University, Weifang, China
[8] Shandong Medical Imaging and Radiotherapy Engineering Center (SMIREC), Shandong Cancer Hospital and Institute, Shandong First Medical University and Shandong Academy of Medical Sciences, Jinan, China

*Xindi Li and Jigang Dong have contributed equally to this work.

Corresponding Author:
Baosheng Li. Department of Radiation Oncology, Shandong Cancer Hospital and Institute, Shandong First Medical University and Shandong Academy of Medical Sciences, No. 440, Jiyan Road, Jinan, China.
Email: bsli@sdfmu.edu.cn

exhibited good predictive performance. **Conclusion:** Our combined model based on Rad-Score and clinical characteristics showed high predictive performance for predicting sensitivity to nCRT in patients with ESCC. It may be useful for predicting treatment effects in clinical practice and demonstrates the significant potential of radiomics in predicting and optimizing treatment decisions.

Introduction

Esophageal cancer is one of the most common malignant tumors, ranking seventh in global incidence and sixth in mortality in 2020, with over 544 000 deaths reported.[1] China has a particularly high incidence of esophageal cancer, accounting for more than half of all cases worldwide,[2] with 90% of these patients suffering from esophageal squamous cell carcinoma (ESCC).[3] Owing to the non-specific early symptoms of esophageal cancer, 80%-90% of patients are diagnosed at an advanced stage and require comprehensive treatment plans.[4] Based on the CROSS and NEOCRTEC5010 studies, neoadjuvant chemoradiotherapy (nCRT) combined with radical resection has become the standard treatment for patients with locally advanced resectable esophageal cancer.[5-7] The CROSS study is the longest-running multicenter randomized controlled trial of nCRT for esophageal cancer. Its results showed that, for patients with locally advanced esophageal cancer, the median overall survival of the patient group who received nCRT combined with surgery was 48.6 months. This was significantly higher than the 24 months in the group who received surgery alone, with a significant benefit in the ESCC population.[5,6] The NEOCRTEC5010 study, a prospective randomized controlled clinical trial conducted at eight large esophageal cancer centers in China, further confirmed the findings of the CROSS study. The results showed that nCRT combined with surgery showed significant advantages in median overall survival and disease-free survival compared with surgery alone, making nCRT the preferred treatment for patients with locally advanced ESCC.[7]

Some patients with ESCC who undergo surgery after nCRT still experience local recurrence and distant metastasis, at rates of up to 33.7%–48%.[8,9] The pathological complete response (pCR) rate of nCRT is only 43.2%–49%,[8,9] and the heterogeneity of treatment responses among patients reflects the complexity of esophageal cancer. This indicates that evidence-based treatment plans may not be well suited for all patients with ESCC, posing a considerable challenge for clinicians. Therefore, identifying patients with ESCC who are sensitive to nCRT would enable clinicians to provide timely and more specific interventions for patients at high risk of tumor control failure and avoid unnecessary treatment for low-risk patients.

Radiomics is an emerging quantitative image analysis method that uses digitalized, quantitative, and high-throughput analysis of imaging modalities—such as computed tomography (CT), magnetic resonance imaging (MRI), and positron emission tomography-CT (PET/CT). Researchers can delineate regions of interest (ROIs) and convert them into imaging features such as intensity, texture, shape, and wavelet transformation using machine learning technology. These feature data are then subjected to dimensionality reduction and normalization to select meaningful radiomics features. Finally, radiomic labels are established through linear or nonlinear machine learning methods, enabling comprehensive quantitative descriptions of the tumors. Radiomics, a technique that converts high-dimensional medical imaging data into quantitative features, has been applied to tumor molecular classification, differential diagnosis, efficacy detection, and prognostic evaluation, providing important assistance in precision oncology clinical decision-making.[10-13] Radiomics can serve as a potential tumor biomarker, providing a more comprehensive description of potential tumor phenotypes by extracting imaging features. The main imaging methods for evaluating esophageal cancer include CT, MRI, and PET/CT. CT is currently the most commonly used method, playing an important role in the diagnosis, staging, treatment guidance, and follow-up of esophageal cancer. MRI is of great value in the diagnosis of mediastinal lymph node metastasis of esophageal cancer. However, owing to interference from heart movement and gastric motility artifacts, as well as the long acquisition time that requires high patient compliance, MRI is not currently recommended for routine imaging of esophageal cancer. PET/CT is also not routinely recommended, because of its high cost, radiation exposure, and inability to detect subtle metastases. Therefore, this study aims to conduct further research based on CT radiomics. To date, radiomics analysis based on CT, MRI, and PET/CT has shown good predictive value in terms of the efficacy, treatment response, prognosis, and lymph node metastasis of esophageal cancer.[14-18] However, few studies have used CT radiomics combined with clinical parameters to predict sensitivity to nCRT in patients with ESCC.

The nCRT approach serves as a crucial therapeutic modality for ESCC. Predicting its efficacy is therefore vital for constructing personalized treatment plans. However, there is still a lack of an accurate and reliable predictive method to assess the sensitivity of patients to nCRT in clinical practice. Studies based on CT radiomics combined with clinical features can improve prediction accuracy. By extracting

quantitative features and combining them with machine learning algorithms, CT radiomics can construct more precise predictive models. These features can reflect the heterogeneity within tumors and thus predict their responses to nCRT. Compared with relying solely on clinical features, combining CT radiomics features can significantly improve the accuracy and reliability of prediction. By predicting a patient's sensitivity to nCRT, physicians can develop more personalized treatment plans for patients, and for those who are predicted to be sensitive, the current treatment regimen can be continued or intensified. Conversely, for those predicted to be insensitive to nCRT, treatment strategies can be adjusted to reduce unnecessary examinations and treatment costs while mitigating the risk of treatment delays and adverse effects.

Therefore, this retrospective study intended to establish a comprehensive model by extracting and analyzing the preoperative CT radiological features of patients with ESCC who received nCRT, combined with clinical parameters, to identify the optimal predictive model for patients with ESCC undergoing nCRT. The goal was to predict sensitivity to nCRT in cases of ESCC before treatment, with the aim of providing risk stratification and decision-making recommendations for clinical treatment plans, as well as offering valuable information for constructing personalized treatment plans.

Methods

Research Participants

Inclusion and Exclusion Criteria. This retrospective study selected 102 consecutive patients with pathologically confirmed ESCC from Shandong Cancer Hospital between 2016 and 2021. All of the patients received standard nCRT before surgery. The study was approved by the Ethics Committee of Shandong Cancer Hospital and Institute, affiliated with Shandong First Medical University, which waived the requirement for informed consent due to the retrospective nature if the study. The workflow of the study is shown in Figure 1.

The main inclusion criteria were as follows: ESCC confirmed by pathological tissue examination through endoscopy; patients evaluated by both the Radiation Oncology and Surgical Oncology Departments who were identified as high risk for surgery and were thus recommended to receive nCRT first; patients assessed to be feasible for surgical treatment after nCRT; patients with no prior radiation, chemotherapy, or other anti-tumor treatments before CT examination; those with availability of clear CT images before treatment; and those for whom complete clinical information was accessible through the medical record system.

The main exclusion criteria were as follows: patients who received only radiotherapy and chemotherapy and did not undergo surgical treatment later on; those with incomplete clinical case information (eg, missing baseline clinical data); and those for whom the CT imaging quality did not meet our required standards.

Treatment Protocol

The medical records of all included patients, who underwent radical surgery after nCRT, were reviewed. The radiotherapy techniques used were intensity-modulated radiotherapy and three-dimensional (3D) conformal radiotherapy. The radiation fractionation scheme was 1.8-2 Gy per fraction, administered once daily, 5 days per week. The chemotherapy regimen consisted of paclitaxel or 5-fluorouracil combined with platinum-based drugs. Each patient received 4-6 cycles of chemotherapy, with each cycle lasting 21 days. The dosage and total number of chemotherapy cycles were adjusted based on each patient's condition, while adhering to the recommendations of the Chinese Society of Clinical Oncology and the National Comprehensive Cancer Network guidelines. Surgical procedures included either three-incision radical esophagectomy (neck, chest, and abdomen) or two-incision radical esophagectomy (chest and abdomen).

Grouping

Based on their pathological results after esophageal cancer resection surgery, the patients were divided into two groups: the chemoradiotherapy-sensitive group, which included patients who achieved pCR; and the chemoradiotherapy-resistant group, which included patients who did not achieve pCR. pCR was defined as the absence of both residual invasive disease and positive lymph nodes in all layers of the esophagus in the surgical specimen after treatment (ypT0N0).

Clinical Model Construction

The patient data collected before treatment included the following parameters: sex, age, smoking history, alcohol history, height, body surface area, weight, Karnofsky performance status score, tumor location, clinical T stage, clinical N stage, clinical tumor, node, and metastasis (TNM) staging, radiation dose, neoadjuvant chemotherapy regimen, operative approach, white blood cell count, lymphocyte count, neutrophil count, platelet-to-lymphocyte ratio, platelet-to-monocyte ratio, lymphocyte-to-monocyte ratio, systemic immune-inflammation index, peripheral blood mononuclear cells, eosinophils, basophils, red blood cell count, hemoglobin level, platelet count, carcinoembryonic antigen (CEA) level, neutrophil-to-lymphocyte ratio (NLR), fibrinogen (FIB) level, cytokeratin 19 fragment level, prothrombin time, thrombin time, activated partial thromboplastin time, D-dimer level, serum aspartate aminotransferase to alanine aminotransferase ratio (S/L), total protein, albumin, globulin, albumin-to-globulin ratio, prealbumin, alkaline phosphatase, cystatin C, and lactate dehydrogenase level. Clinical T-stage and N-stage were assessed according to the eighth edition of the TNM staging system for esophageal and esophagogastric junction cancers by the Union for International Cancer Control and the American Joint Committee on Cancer. Univariate analysis was
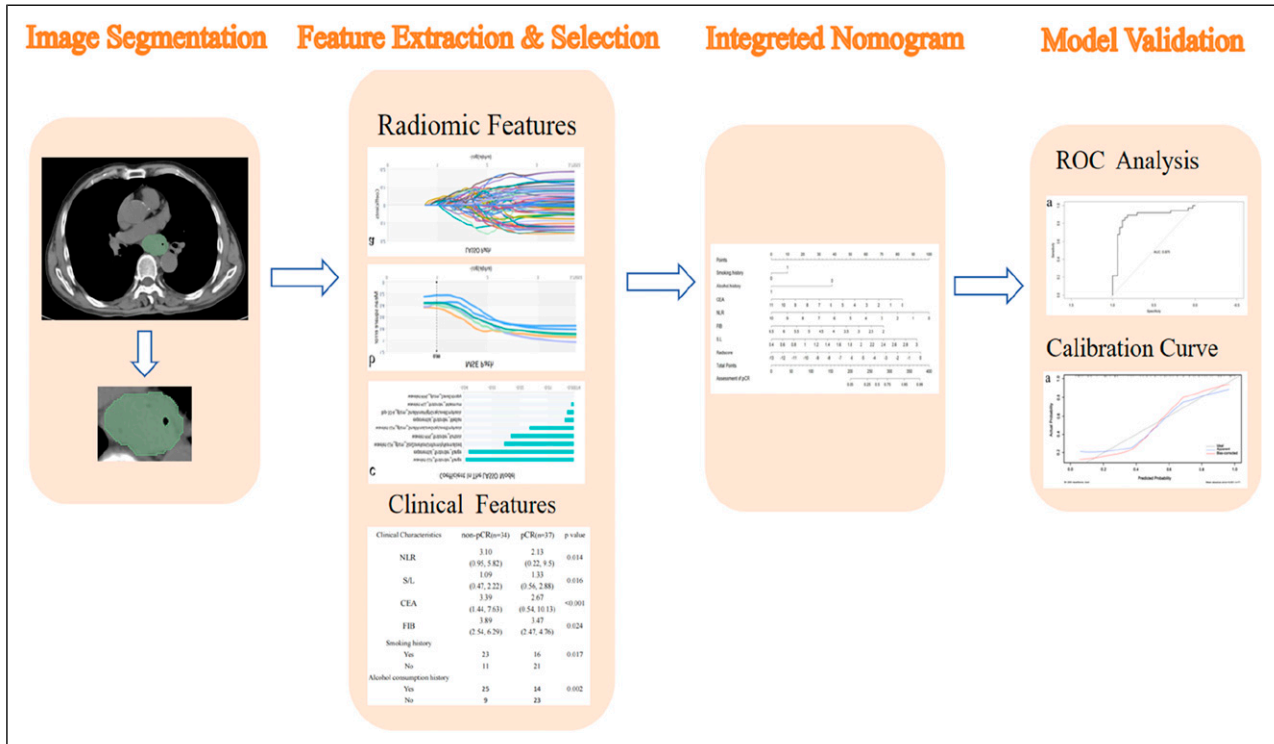
Figure 1. Workflow of the study.

performed to assess the relationship between clinical features and sensitivity to nCRT in patients with ESCC. Clinical variables with *P* values <0.05 were used to develop a clinical model for predicting sensitivity to nCRT.

Radiomics Analysis

Image Segmentation. CT images taken within 1 month before nCRT were collected and uploaded to the RadCloud radiomics platform (https://radcloud.cn/). Two doctors with over 5 years of experience in chest imaging diagnosis independently used the 3D-Slicer software to delineate the ROIs on the CT images, outlining the primary esophageal tumor while avoiding vascular bundles, fat, calcifications, the esophageal lumen, and surrounding organs. For validation, 20 randomly selected patients were reassessed by two experienced radiologists for repeated segmentation. The inter-observer consistency coefficient was calculated based on the results of the two radiomics feature extractions, and an inter-observer consistency coefficient of >0.75 was considered to indicate good robustness and reproducibility. We performed a consistency check and found good agreement between the ROI delineations of the two radiologists.

Feature Extraction and Selection. Radiomics features were extracted from the ROIs using the RadCloud platform (https://radcloud.cn/). In total, 1688 radiomics features were extracted from the CT images of each patient. These features were classified into three categories. The first group (first-order statistics)

consisted of 126 descriptors that quantitatively characterized the voxel intensity distribution within the CT images using common basic metrics. The second group (shape- and size-based features) included 14 3D features reflecting the shape and size of the region. The third group (textural features) comprised 525 features that quantified regional heterogeneity differences based on gray-level run length and gray-level co-occurrence matrix calculations.

After radiomics feature extraction, several feature selection methods were used for normalization and dimensionality reduction to ensure consistency in the magnitudes of different features and reduce redundant features. Variance thresholding (at a threshold of 0.8) was used to remove features with variance values <0.8. The SelectKBest method, a univariate feature selection approach, used *P* values to analyze the relationship between features and the classification outcome, and all features with *P* values <0.05 were selected. For the LASSO model, L1 regularization was used as the cost function, with a cross-validation error set to 5 and a maximum number of iterations of 1000.

Construction of Machine Learning Models

The 102 patients with ESCC were randomly divided into training and validation sets in a 7:3 ratio. Based on the radiomics features selected using LASSO regression, a radiomics score (Rad-Score) was calculated by linearly weighting

Table 1. Comparison of Patients' Characteristics Between Training Set and Validation Set.

Clinical Characteristics	Training set (n = 71)	Validation set (n = 31)	P value
Sex			0.963
Female	12	7	
Male	59	24	
Age			0.067
<61	32	8	
>=61	39	23	
Smoking history			0.993
No	32	14	
Yes	39	17	
Alcohol history			0.757
No	32	15	
Yes	39	16	
Height (cm)			0.344
<167	37	13	
>=167	34	18	
BSA (m^2)			0.910
<1.96	69	30	
>=1.96	2	1	
Weight (Kg)			0.551
<62.4	39	19	
>=62.4	32	12	
KPS score			0.493
<85	35	13	
>=85	36	18	
Tumor location			0.829
Distal	36	15	
Middle	25	13	
Middle-Distal	9	3	
Upper	1	0	
Clinical T Stage			0.850
T2	7	2	
T3	60	27	
T4	4	2	
Clinical N Stage			0.392
N0	18	12	
N1	41	15	
N2	12	4	
Clinical Staging			0.547
IIA	9	6	
IIB	8	6	
IIIA	2	1	
IIIB	50	18	
IVA	2	0	
Radiation dose			0.814
1.8 Gy*23	63	27	
2 Gy*20	8	4	
WBC ($\times 10^9$/L)			0.859
<6.75	38	16	
>=6.75	33	15	

(continued)

Table 1. (continued)

Clinical Characteristics	Training set (n = 71)	Validation set (n = 31)	P value
LYM ($\times 10^9$/L)			0.064
<1.73	46	14	
>=1.73	25	17	
NE ($\times 10^9$/L)			0.859
<4.36	38	16	
>=4.36	33	15	
PLR			0.807
<176.08	44	20	
>=176.08	27	11	
PMR			0.859
<560.44	38	16	
>=560.44	33	15	
LMR			0.382
<3.65	41	15	
>=3.65	30	16	
SII			0.879
<774.49	47	21	
>=774.49	24	10	
PBMC ($\times 10^9$/L)			0.811
<0.96	68	30	
>=0.96	3	1	
EOS ($\times 10^9$/L)			0.735
<0.12	46	19	
>=0.12	25	12	
BASO ($\times 10^9$/L)			0.282
<0.04	38	13	
>=0.04	33	18	
RBC ($\times 10^{12}$/L)			0.493
<4.6	36	18	
>=4.6	35	13	
HGB (g/L)			0.382
<143.4	30	16	
>=143.4	41	15	
PLT ($\times 10^9$/L)			0.213
<264.23	34	19	
>=264.23	37	12	
CEA (ng/ml)			0.871
<2.98	40	18	
>=2.98	31	13	
NLR			0.83
<2.53	35	16	
>=2.53	36	15	
FIB (g/L)			0.181
<3.59	38	21	
>=3.59	33	10	
Cyfra21-1 (ng/ml)			0.869
<3.15	47	20	
>=3.15	24	11	
PT (S)			0.467
<10.51	38	19	
>=10.51	33	12	

(continued)

Table 1. (continued)

Clinical Characteristics	Training set (n = 71)	Validation set (n = 31)	P value
TT (S)			0.479
<13.78	42	16	
>=13.78	29	15	
APTT (S)			0.111
<29.98	36	21	
>=29.98	35	10	
D-dimer (mg/L)			0.571
<0.4	52	21	
>=0.4	19	10	
S/L			0.094
<1.26	38	11	
>=1.26	33	20	
TP (g/L)			0.101
<69.94	40	12	
>=69.94	31	19	
ALB (g/L)			0.757
<44.79	32	15	
>=44.79	39	16	
GLB (g/L)			0.607
<25.15	36	14	
>=25.15	35	17	
A/G			0.706
<1.86	43	20	
>=1.86	28	11	
PA (g/L)			0.507
<2.06	70	31	
>=2.06	1	0	
Cys C (mg/L)			0.729
<61	37	15	
>=61	34	16	
LDH (U/L)			0.933
<192.76	36	16	
>=192.76	35	15	

Abbreviations: KPS score, Karnofsky performance status score; WBC, white blood cell; LYM, lymphocyte; NE, neutrophil; PLR, platelet-lymphocyte ratio; PMR, platelet-to-monocyte ratio; LMR, lymphocyte-to-monocyte ratio; SII, systemic immune-inflammation index; PBMC, peripheral blood mononuclear cell; EOS, eosinophils; BASO, basophils; RBC, red blood cell; HGB, hemoglobin; PLT, platelet. CEA, carcinoembryonic antigen; NLR, neutrophil-to-lymphocyte ratio; FIB, fibrinogen; CYFRA21-1, cytokeratin-19 fragment; PT, prothrombin time; TT, thrombin time; APTT, activated partial thromboplastin time; S/L, serum aspartate aminotransferase to alanine aminotransferase ratio; TP, total protein; ALB, albumin; GLB, globulin; A/G, albumin/globulin ratio; PA, prealbumin; Cys C, cystatin C; LDH, lactate dehydrogenase.

the corresponding coefficient values. The formula used for the radiomics model was:

$$Rad - Score = \alpha + n\sum_{i=1}^{n}\beta iXi$$

where α represents the intercept, βi the value of the radiomics feature, and Xi the corresponding coefficient.

In this study, eight classifiers—including K-nearest neighbors (KNN), support vector machine (SVM), extreme gradient boost (XGBoost), linear discriminant analysis (LDA), logistic regression (LR), Bernoulli Naive Bayes (BernoulliNB), multi-layer perceptron classifier (MLPClassifier), and stochastic gradient descent (SGD)—were used to construct the radiomics models. To evaluate the predictive performance of the models, area under the curve (AUC) values were calculated for both the training and validation datasets. Four indicators were used to evaluate the performance of the classifiers in this study: P (precision = true positives/[true positives + false positives]), R (recall = true positives/[true positives + false negatives]), F1-score (F1-score = P × R × 2/[P + R]), and support (total number in the test set).

Construction of the Combined Model

The clinical variables with *P* values <0.05 selected through univariate analysis and Rad-Score were included in our model. A combined model was established based on binary logistic regression, and a nomogram was developed to present the predicted probabilities of the outcomes visually. The performance of the combined model was evaluated using receiver operating characteristic (ROC) and calibration curves.

Statistical Analysis

The radiomics statistical analysis in this study was conducted using the RadCloud platform. Statistical analysis of the clinical factors was performed using SPSS 27.0 (IBM Corp.). Continuous variables were tested for normality. Those that conformed to a normal distribution were compared using independent samples Student's ttest, whereas those that did not were compared using the Mann-Whitney U test. Categorical variables were compared between groups using the chi-squared test. Statistical significance was set at p < 0.05. Nomograms, ROC curves, and calibration curves were generated using R version 3.6.0 for further analysis. This research writing follows the STROBE guidelines.

Results

General Information

In total, 102 patients with ESCC who underwent nCRT were included in this study. The patients were randomly divided into training and validation sets in a 7:3 ratio, with 71 and 31 patients in the training and validation sets, respectively. No significant differences were observed in the general information between the training and validation sets (p > 0.05; Table 1).

Extraction of Radiomics Features and Establishment of Rad-Score

Based on the CT images, we first filtered 1688 radiomics features using the variance method and then applied the optimal selection
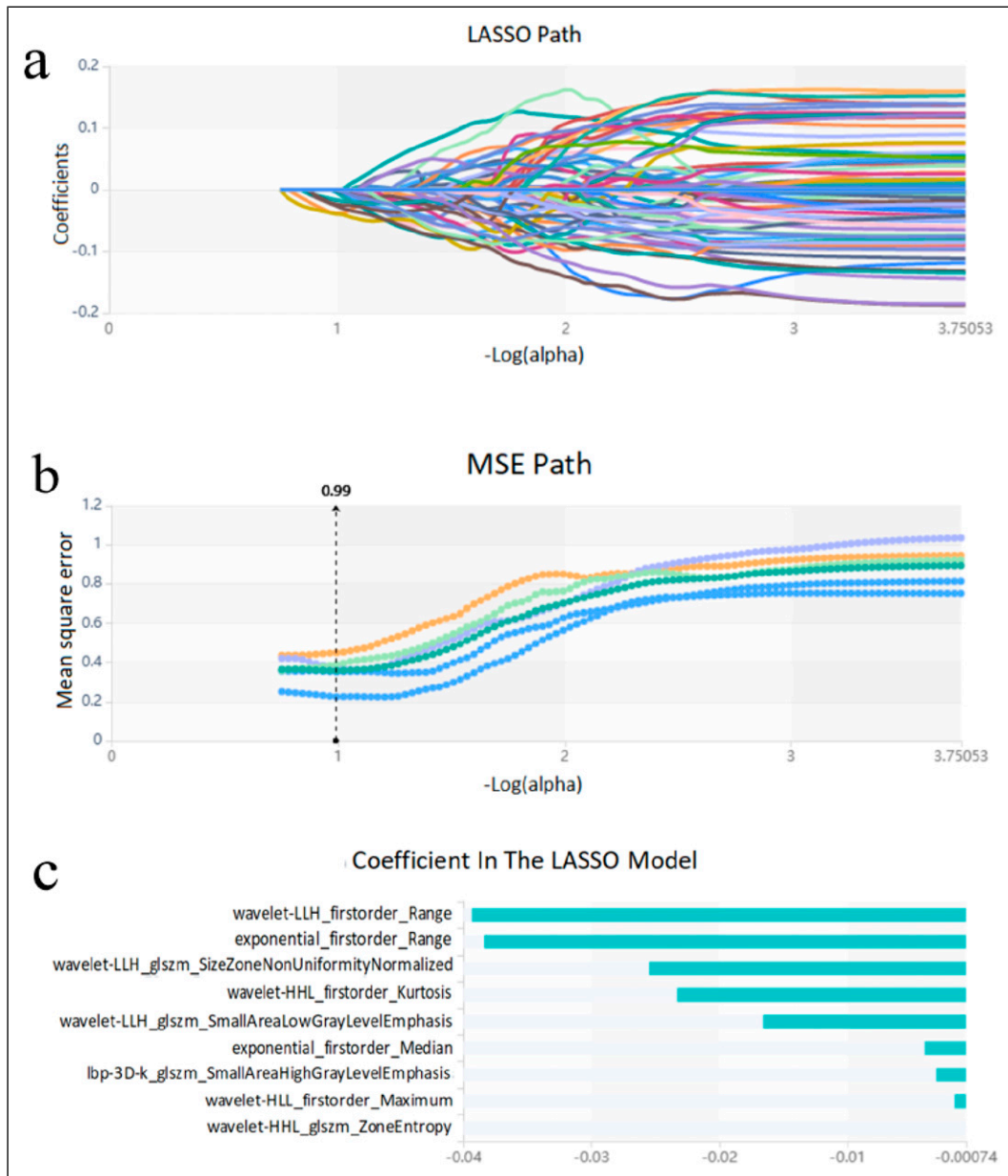
Figure 2. LASSO algorithm on feature selected. (A) LASSO path; (B) MSE path; (C) Coefficients in the LASSO model. Using the LASSO model, nine features that correspond to the optimal alpha value were selected.

method K for further filtering. In the end, nine optimal features were selected using the LASSO algorithm (Figure 2), and a radiomics label (Rad-Score) was constructed (Table 2).

Table 3 summarizes the evaluation results of 8 classifiers using different feature sets extracted from CT images, with SVM being the most effective classifier.

Clinical Characteristics

Univariate analysis was performed on the clinical characteristics of patients in the training set. As shown in Table 4, smoking and alcohol history, NLR, S/L, CEA, and FIB were identified as factors influencing the sensitivity of ESCC to nCRT. A clinical model was constructed on the basis of these independent predictors.

Construction and Validation of the Combined Model

Univariate analysis revealed a significant difference in Rad-Score between the two groups of patients ($p < 0.05$). Combined with clinical features (smoking history, alcohol history, NLR, S/L, CEA, and FIB) with P values of <0.05, a combined model was constructed based on binary logistic regression. A

Table 2. Descriptions of Selected Radiomics Features and Their Associated Feature Groups and Filters.

Radiomics Feature	Radiomics Class	Filter
Median	Firstorder	Exponential
Range	Firstorder	Exponential
SmallAreaHighGrayLevelEmphasis	Glszm	Lbp-3D-k
Maximum	Firstorder	Wavelet-HLL
Range	Firstorder	Wavelet-LLH
SizeZoneNonUniformityNormalized	Glszm	Wavelet-LLH
SmallAreaLowGrayLevelEmphasis	Glszm	Wavelet-LLH
Kurtosis	Firstorder	Wavelet-HHL
ZoneEntropy	Glszm	Wavelet-HHL

Table 3. Evaluation Metrics for 8 Classifiers on Training Set and Validation Set.

	Classifiers	AUC	95% CI	Sensitivity	Precision	F1-score	Support
Training set	SVM	0.937	0.856 - 1.000	0.840	0.890	0.860	37
	XGBoost	0.998	0.972 - 1.000	0.970	1.000	0.990	37
	KNN	0.892	0.808 - 0.976	0.760	0.900	0.820	37
	BernoulliNB	0.806	0.702 - 0.910	0.700	0.740	0.720	37
	LDA	0.841	0.751 - 0.931	0.810	0.830	0.820	37
	LR	0.847	0.754 - 0.940	0.780	0.830	0.810	37
	SGD	0.824	0.725 - 0.923	0.760	0.780	0.770	37
	MLPClassifier	0.986	0.937 - 1.000	0.970	0.950	0.960	37
Validation set	SVM	0.831	0.679 - 0.983	0.810	0.760	0.790	16
	XGBoost	0.800	0.630 - 0.970	0.690	0.690	0.690	16
	KNN	0.790	0.635 - 0.945	0.810	0.760	0.790	16
	BernoulliNB	0.804	0.645 - 0.963	0.690	0.790	0.730	16
	LDA	0.754	0.604 - 0.904	0.690	0.790	0.730	16
	LR	0.742	0.591 - 0.893	0.690	0.790	0.730	16
	SGD	0.754	0.606 - 0.902	0.750	0.800	0.770	16
	MLPClassifier	0.746	0.588 - 0.904	0.750	0.710	0.730	16

Abbreviations: AUC, area under the curve; SVM, support vector machine; KNN, K-nearest neighbors; XGBoost, extreme gradient boost; LDA, linear discriminant analysis; LR, logistic regression; BernoulliNB, Bernoulli Naive Bayes; MLPClassifier, multi-layer perceptron classifier; SGD, stochastic gradient descent.

nomogram (Figure 3) was created, and the performance of the model was evaluated using ROC and calibration curves. The AUCs of the combined model for the validation and training sets were 0.821 and 0.870, respectively. The calibration curve showed that the nomogram's predictions were relatively close to the actual clinical observations. The ROC and calibration curves of the combined model are shown in Figures 4 and 5.

Discussion

In this study, we developed and validated a combined model based on CT radiomics and clinical parameters, which effectively predicted the sensitivity of nCRT in patients with ESCC using machine learning methods. It may provide a potentially effective, non-invasive, practical, and reliable method for predicting the sensitivity of nCRT in ESCC patients, thereby offering clinicians with supporting information for clinical decision-making.

One of the hallmarks of malignant tumors is their heterogeneity, which is associated with their malignant biological behaviors.[19,20] Radiomics can reveal microscopic tumor information that is undetectable in naked-eye analyses of two-dimensional (2D) medical images, quantifying the internal spatiotemporal heterogeneity of tumors.[21,22] This information includes cell infiltration, necrosis of fine structures, and abnormal angiogenesis. These factors can also reflect tumor glucose metabolism and angiogenesis status to some degree.[12,23-26] A large number of previous studies have demonstrated the application of radiomic features in predicting the treatment response of nCRT in patients with ESCC. Liu Y et al established a model to predict pCR to nCRT in ESCC by combining magnetic resonance radiomics and dynamic hemodynamics.[27] The research teams of Liu Y and Lu S both established MRI-based radiomic models to accurately predict the pathological response of ESCC patients after receiving nCRT.[28,29] Kasai A et al developed a CT-based radiomic model combined with artificial intelligence (AI)

Table 4. Univariate Analyses of Variables Linked to pCR in Patients With ESCC.

Clinical Characteristics	Non-pCR(n = 34)	pCR(n = 37)	P value
NLR	3.10 (0.95, 5.82)	2.13 (0.22, 9.5)	0.014
S/L	1.09 (0.47, 2.22)	1.33 (0.56, 2.88)	0.016
CEA	3.39 (1.44, 7.63)	2.67 (0.54, 10.13)	<0.001
FIB	3.89 (2.54, 6.29)	3.47 (2.47, 4.76)	0.024
Smoking history			0.017
Yes	23	16	
No	11	21	
Alcohol history			0.002
Yes	25	14	
No	9	23	

Values are presented as means. Abbreviations: KNN, K-nearest neighbors; SVM, support vector machine; XGBoost, extreme gradient boost; LDA, linear discriminant analysis; LR, logistic regression; BernoulliNB, Bernoulli naive Bayes; MLPClassifier, multi-layer perceptron classifier; SGD, stochastic gradient descent.
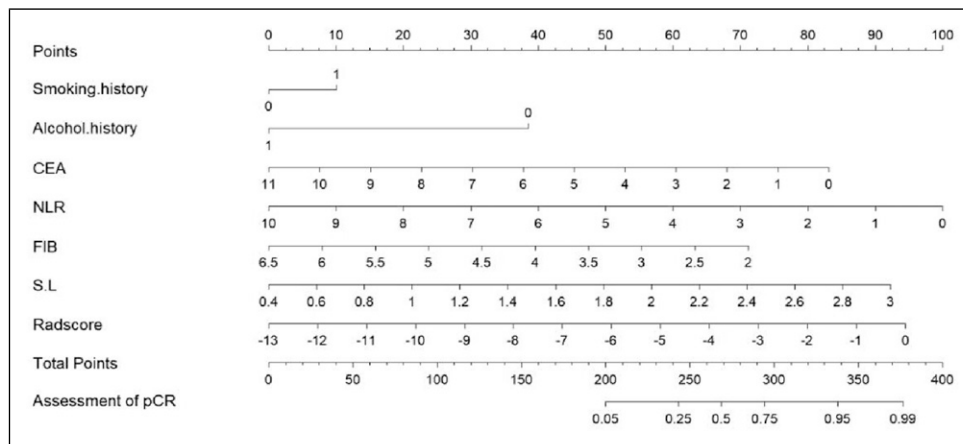
Figure 3. The visual nomogram in the combined model.

technology to predict the response and prognosis of patients with ESCC to chemoradiotherapy.[30] For patients with locally advanced ESCC, when nCRT combined with esophagectomy is used as the standard treatment, many researchers have explored neoadjuvant immunotherapy. Wang JL et al established and validated a radiomic model based on enhanced CT images combined with clinical data to predict the major pathological response of patients with ESCC to neoadjuvant immunotherapy.[18] CT is the primary imaging modality used during clinical staging and therapeutic response assessment for esophageal cancer. This study primarily investigated CT-based radiomics in ESCC by extracting 1688 radiomics features from the ROIs on plain CT images, including first-order statistics, shape, size, and texture features. These features cover one-dimensional, 2D, and 3D characteristics, and comprehensively describe the tumor characteristics in CT images. We analyzed the correlation between these radiomics features and the sensitivity of ESCC to nCRT. Nine relatively important radiomics features, including five first-order features and four gray-level size zone matrix features were

identified. First-order features represent the distribution of voxel intensities in the image, whereas the gray-level size zone matrix comprises texture features representing the spatial characteristics or voxel intensity distribution of the image gray levels, providing information on the relative positions of different gray levels in the image. After feature selection, we utilized eight classifiers to construct a radiomics model to evaluate the maximal effect of CT radiomics in predicting the sensitivity of ESCC to nCRT, and selected the most suitable algorithm for fitting radiomics features. The results showed that all eight classifiers exhibited high AUC values, with SVM being the most effective classifier. These high AUC values indicate that the CT radiomics model has a strong potential for clinical application as a tool for predicting patient response to nCRT.

Furthermore, this study screened six clinical factors that were found to be associated with the sensitivity of ESCC to nCRT (NLR, S/L, CEA, FIB, and smoking and alcohol history), and a clinical model was established based on these factors. The NLR, the ratio of neutrophils to lymphocytes,
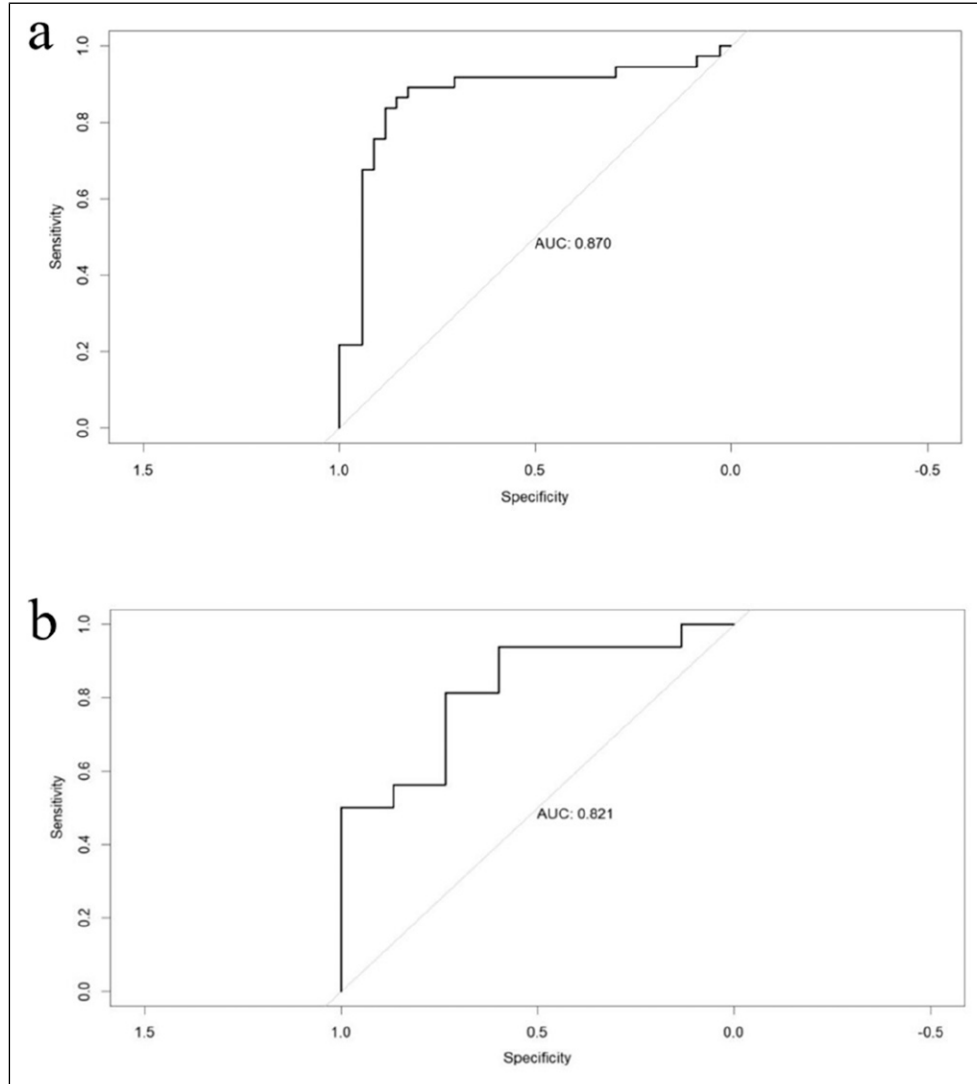
Figure 4. ROC curve analysis for the nomogram. (A) Combined model in training set; (B) Combined model in validation set.

reflects the balance of these two inflammation-related cells and can reflect the inflammatory response in the body. Changes in this value may reflect alterations in the tumor microenvironment. Systemic inflammation is an important feature of malignant tumors that may significantly affect tumor initiation and progression, as well as their invasive and metastatic capabilities. Recent studies have found that an elevated NLR is associated with poor prognosis in many tumors[31] and can reflect the sensitivity of patients with tumors to treatment.[32,33] S/L, which is the ratio of AST to ALT, represents two enzymes that are involved in various biochemical metabolic pathways of cells and are commonly used indicators to reflect liver function. Elevated S/L ratios represent high oxidative stress and an inflammatory environment in the body. Oxidative stress and inflammation are closely related to cancer development.[34,35] The S/L ratio is an independent prognostic factor for malignancies such as prostate and bladder cancer.[36,37] CEA is an acidic glycoprotein present on the

surfaces of cancer cells that exists as a membrane structural protein with human embryonic antigen characteristics. It is a broad-spectrum tumor marker that can be used for disease monitoring, therapeutic response evaluation, and the prognostic assessment of various malignancies.[38-41]

FIB, a plasma protein synthesized in the liver, is an important indicator of coagulation function.[42] Changes in FIB levels reflect abnormal activation of the coagulation system. A number of studies have shown that a hypercoagulable state is associated with tumor invasion and metastasis.[43,44] An abnormal coagulation status can also affect the generation and function of immunosuppressive cells, leading to abnormal functions of regulatory T cells, tumor-associated macrophages, and other immunosuppressive cells—thus providing immune escape mechanisms for tumor cells.[45,46] Smoking and alcohol consumption represent high risk factors for esophageal cancer. Tobacco contains carcinogens such as aromatic amines, aldehydes, phenols, and nitrosamines,
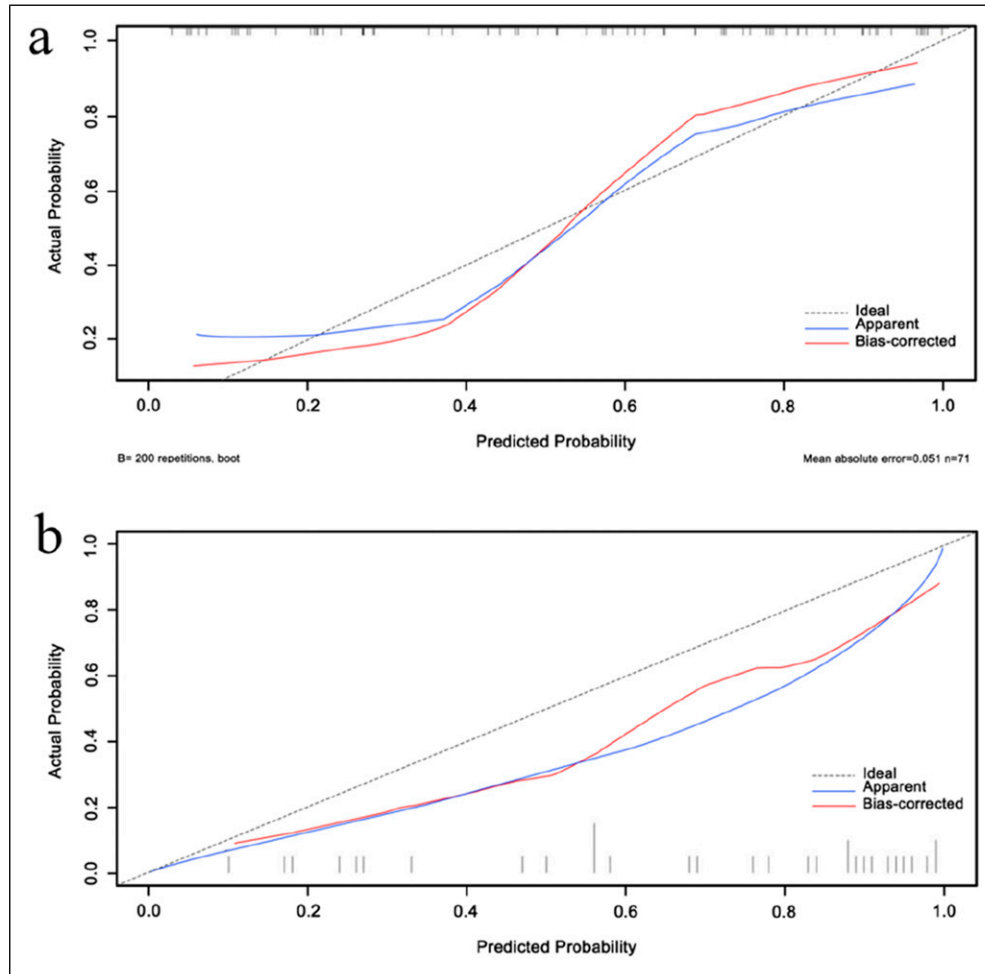
Figure 5. Calibration curve analysis for the nomogram. (A) Combined model in training set; (B) Combined model in validation set.

which can affect the development of esophageal cancer when passing through the esophagus.[47] The main component of alcohol is ethanol, which is oxidized to acetaldehyde by alcohol dehydrogenase in the liver, then metabolized to acetic acid by acetaldehyde dehydrogenase. Ethanol and acetaldehyde can enter esophageal epithelial cells through local infiltration or systemic circulation, exerting direct carcinogenic effects. When smoking and alcohol consumption exceed certain levels, the risk of esophageal cancer increases significantly.[48]

In this study, these six clinical factors were combined with the Rad-Score to construct a combined model, upon which a nomogram model was then developed. The predictive performance of the combined model was evaluated using ROC and calibration curves. The results showed that the combined model exhibited good predictive performance, with an AUC value of 0.870 in the training set and 0.821 in the validation set. The calibration curve demonstrated appropriate goodness of fit for the combined model. Overall, we have successfully developed a combined predictive model for assessing the sensitivity of patients with ESCC to nCRT and it has

demonstrated good predictive performance in both training and validation sets.

Despite our promising results, this study had certain limitations. First, this was a retrospective study with a relatively small sample size, and no sample size analysis and calculation were performed. The applicability of the model requires further validation in a larger sample. Second, this study established an esophageal cancer prediction model using radiomics, identifying 9 features from the 1688 extracted features related to treatment efficacy and deriving a linear regression equation. However, because of the small number of cases in this study, it may lead to overfitting in linear analysis, thereby affecting prediction accuracy. In addition, interpreting the relationship between these features and tumor biological characteristics remains an issue to be resolved. Finally, there are standardization issues with CT image data across different hospitals and equipment, which can affect the extraction of radiomics features and the generalization ability of the model. The current research is still in its preliminary stage and requires validation and application in larger-scale, multi-center clinical trials.

Conclusion

Our combined model based on CT radiomics and clinical parameters showed good performance for predicting the sensitivity of patients with ESCC to nCRT. This model can effectively provide risk stratification and inform decision-making for clinical treatment. By providing information tailored to each patient's unique circumstances, this can enhance personalized therapy.

Ethical Statement

Ethical Approval

This retrospective study was conducted according to the guidelines of the Declaration of Helsinki, and was approved by the Clinical Research Ethics Committee of Shandong Cancer Hospital and Institute (approval number: SDTHEC2024004034). The requirement for informed consent was waived by the ethics committee. All of the authors confirm that all of the procedures were carried out following the relevant guidelines and regulations.

ORCID iDs

Xindi Li https://orcid.org/0009-0003-3196-7097
Baosheng Li https://orcid.org/0009-0009-5351-1502

References

1. Sung H, Ferlay J, Siegel RL, et al. Global cancer statistics 2020: GLOBOCAN estimates of incidence and mortality worldwide for 36 cancers in 185 countries. *CA Cancer J Clin*. 2021;71(3): 209-249. doi:10.3322/caac.21660

2. GBD 2017 Oesophageal Cancer Collaborators. The global, regional, and national burden of oesophageal cancer and its attributable risk factors in 195 countries and territories, 1990-2017: a systematic analysis for the Global Burden of Disease Study 2017. *Lancet Gastroenterol Hepatol*. 2020;5(6):582-597. doi:10.1016/S2468-1253(20)30007-8

3. Global Burden of Disease 2019 Cancer Collaboration,Kocarnik JM, Compton K, et al. Cancer incidence, mortality, years of life lost, years lived with disability, and disability-adjusted life years for 29 cancer groups from 2010 to 2019: a systematic analysis for the Global Burden of Disease Study 2019. *JAMA Oncol*. 2022;8(3):420-444. doi:10.1001/jamaoncol.2021.6987

4. Ajani JA, D'Amico TA, Bentrem DJ, et al. Esophageal and esophagogastric junction cancers, version 2.2019, NCCN clinical practice guidelines in oncology. *J Natl Compr Canc Netw*. 2019;17(7):855-883. doi:10.6004/jnccn.2019.0033

5. Shapiro J, van Lanschot JJB, Hulshof MCCM, et al. Neoadjuvant chemoradiotherapy plus surgery versus surgery alone for oesophageal or junctional cancer (CROSS): long-term results of a randomised controlled trial. *Lancet Oncol*. 2015;16(9): 1090-1098. doi:10.1016/S1470-2045(15)00040-6

6. van Hagen P, Hulshof MC, van Lanschot JJ, et al. Preoperative chemoradiotherapy for esophageal or junctional cancer. *N Engl J Med*. 2012;366(22):2074-2084. doi:10.1056/NEJMoa1112088

7. Yang H, Liu H, Chen Y, et al. Neoadjuvant chemoradiotherapy followed by surgery versus surgery alone for locally advanced squamous cell carcinoma of the esophagus (NEOCRTEC5010): a phase III multicenter, randomized, open-label clinical trial. *J Clin Oncol*. 2018;36(27):2796-2803. doi:10.1200/JCO.2018.79.1483

8. Eyck BM, van Lanschot JJB, Hulshof MCCM, et al. Ten-year outcome of neoadjuvant chemoradiotherapy plus surgery for esophageal cancer: the randomized controlled CROSS trial. *J Clin Oncol*. 2021;39(18):1995-2004. doi:10.1200/JCO.20. 03614

9. Liu S, Wen J, Yang H, et al. Recurrence patterns after neoadjuvant chemoradiotherapy compared with surgery alone in oesophageal squamous cell carcinoma: results from the multicenter phase III trial NEOCRTEC5010. *Eur J Cancer*. 2020; 138:113-121. doi:10.1016/j.ejca.2020.08.002

10. Gao D, Tan BG, Chen XQ, et al. Contrast-enhanced CT radiomics features to preoperatively identify differences between tumor and proximal tumor-adjacent and tumor-distant tissues of resectable esophageal squamous cell carcinoma. *Cancer Imag*. 2024;24(1):11. doi:10.1186/s40644-024-00656-0

11. Cai M, Song B, Deng Y, et al. Automatically optimized radiomics modeling system for small gastric submucosal tumor (<2 cm) discrimination based on EUS images. *Gastrointest Endosc*. 2024;99(4):537-547. doi:10.1016/j.gie.2023.11.006

12. Wang X, Xie T, Luo J, Zhou Z, Yu X, Guo X. Radiomics predicts the prognosis of patients with locally advanced breast cancer by reflecting the heterogeneity of tumor cells and the tumor microenvironment. *Breast Cancer Res*. 2022;24(1):20. doi:10. 1186/s13058-022-01516-0

13. Liu Z, Wang S, Dong D, et al. The applications of radiomics in precision diagnosis and treatment of oncology: opportunities and challenges. *Theranostics*. 2019;9(5):1303-1322. doi:10. 7150/thno.30309

14. Wang JL, Tang LS, Zhong X, et al. A machine learning radiomics based on enhanced computed tomography to predict neoadjuvant immunotherapy for resectable esophageal squamous cell carcinoma. *Front Immunol*. 2024;15:140514. doi:10.3389/fimmu.2024.1405146

15. Fan L, Yang Z, Chang M, Chen Z, Wen Q. CT-based delta-radiomics nomogram to predict pathological complete response after neoadjuvant chemoradiotherapy in esophageal squamous cell carcinoma patients. *J Transl Med*. 2024;22(1):579. doi:10.1186/s12967-024-05392-4

16. Qu J, Ma L, Lu Y, et al. DCE-MRI radiomics nomogram can predict response to neoadjuvant chemotherapy in esophageal cancer. *Discov Oncol*. 2022;13(1):3. doi:10.1007/s12672-022-00464-7

17. Zhang C, Shi Z, Kalendralis P, et al. Prediction of lymph node metastases using pre-treatment PET radiomics of the primary tumour in oesophageal adenocarcinoma: an external validation study. *Br J Radiol*. 2021;94(1118):20201042. doi:10.1259/bjr.20201042

18. Guo H, Tang HT, Hu WL, et al. The application of radiomics in esophageal cancer: predicting the response after neoadjuvant therapy. *Front Oncol*. 2023;13:1082960. doi:10.3389/fonc.2023.1082960

19. Kashyap A, Rapsomaniki MA, Barros V, et al. Quantification of tumor heterogeneity: from data acquisition to metric generation. *Trends Biotechnol*. 2022;40(6):647-676. doi:10.1016/j.tibtech.2021.11.006

20. Zhang C, Guan Y, Sun Y, Ai D, Guo Q. Tumor heterogeneity and circulating tumor cells. *Cancer Lett*. 2016;374(2):216-223. doi:10.1016/j.canlet.2016.02.024

21. Su GH, Xiao Y, You C, et al. Radiogenomic-based multiomic analysis reveals imaging intratumor heterogeneity phenotypes and therapeutic targets. *Sci Adv*. 2023;9(40):eadf0837. doi:10.1126/sciadv.adf0837

22. Kang W, Qiu X, Luo Y, et al. Application of radiomics-based multiomics combinations in the tumor microenvironment and cancer prognosis. *J Transl Med*. 2023;21(1):598. doi:10.1186/s12967-023-04437-4

23. Li G, Li L, Li Y, et al. An MRI radiomics approach to predict survival and tumour-infiltrating macrophages in gliomas. *Brain*. 2022;145(3):1151-1161. doi:10.1093/brain/awab340

24. Xu X, Zhang HL, Liu QP, et al. Radiomic analysis of contrast-enhanced CT predicts microvascular invasion and outcome in hepatocellular carcinoma. *J Hepatol*. 2019;70(6):1133-1144. doi:10.1016/j.jhep.2019.02.023

25. Mayerhoefer ME, Riedl CC, Kumar A, et al. Radiomic features of glucose metabolism enable prediction of outcome in mantle cell lymphoma. *Eur J Nucl Med Mol Imaging*. 2019;46(13):2760-2769. doi:10.1007/s00259-019-04420-6

26. Xia TY, Zhou ZH, Meng XP, et al. Predicting microvascular invasion in hepatocellular carcinoma using CT-based radiomics model. *Radiology*. 2023;307(4):222729. doi:10.1148/radiol.222729

27. Liu Y, Ma Z, Bao Y, et al. Integrating MR radiomics and dynamic hematological factors predicts pathological response to neoadjuvant chemoradiotherapy in esophageal cancer. *Heliyon*. 2024;10(13):33702. doi:10.1016/j.heliyon.2024.e33702

28. Lu S, Wang C, Liu Y, et al. The MRI radiomics signature can predict the pathologic response to neoadjuvant chemotherapy in locally advanced esophageal squamous cell carcinoma. *Eur Radiol*. 2024;34(1):485-494. doi:10.1007/s00330-023-10040-4

29. Liu Y, Wang Y, Wang X, et al. MR radiomics predicts pathological complete response of esophageal squamous cell carcinoma after neoadjuvant chemoradiotherapy: a multicenter study. *Cancer Imag*. 2024;24(1):16. doi:10.1186/s40644-024-00659-x

30. Kasai A, Miyoshi J, Sato Y, et al. A novel CT-based radiomics model for predicting response and prognosis of chemoradiotherapy in esophageal squamous cell carcinoma. *Sci Rep*. 2024;14(1):2039. doi:10.1038/s41598-024-52418-4

31. Cupp MA, Cariolou M, Tzoulaki I, Aune D, Evangelou E, Berlanga-Taylor AJ. Neutrophil to lymphocyte ratio and cancer prognosis: an umbrella review of systematic reviews and meta-analyses of observational studies. *BMC Med*. 2020;18(1):360. doi:10.1186/s12916-020-01817-1

32. Valero C, Lee M, Hoen D, et al. Pretreatment neutrophil-to-lymphocyte ratio and mutational burden as biomarkers of tumor response to immune checkpoint inhibitors. *Nat Commun*. 2021;12(1):729. doi:10.1038/s41467-021-20935-9

33. Chen MF, Chen PT, Kuan FC, Chen WC. The predictive value of pretreatment neutrophil-to-lymphocyte ratio in esophageal squamous cell carcinoma. *Ann Surg Oncol*. 2019;26(1):190-199. doi:10.1245/s10434-018-6944-1

34. Taniguchi K, Karin M. NF-κB, inflammation, immunity and cancer: coming of age. *Nat Rev Immunol*. 2018;18(5):309-324. doi:10.1038/nri.2017.142

35. Wu J, Chen L, Wang Y, Tan W, Huang Z. Prognostic value of aspartate transaminase to alanine transaminase (De Ritis) ratio in solid tumors: a pooled analysis of 9,400 patients. *OncoTargets Ther*. 2019;12:5201-5213. doi:10.2147/OTT.S204403

36. Zhou J, He Z, Ma S, Liu R. AST/ALT ratio as a significant predictor of the incidence risk of prostate cancer. *Cancer Med*. 2020;9(15):5672-5677. doi:10.1002/cam4.3086

37. Ghahari M, Salari A, Ghafoori Yazdi M, et al. Association between preoperative De Ritis (AST/ALT) ratio and oncological outcomes following radical cystectomy in Patients with Urothelial Bladder Cancer. *Clin Genitourin Cancer*. 2022;20(2):e89-e93. doi:10.1016/j.clgc.2021.10.007

38. Yousef A, Yousef M, Zeineddine MA, et al. Serum tumor markers and outcomes in patients with appendiceal adenocarcinoma. *JAMA Netw Open*. 2024;7(2):e240260. doi:10.1001/jamanetworkopen.2024.0260

39. Fakih M, Sandhu J, Wang C, et al. Evaluation of comparative surveillance strategies of circulating tumor DNA, imaging, and carcinoembryonic antigen levels in patients with resected colorectal cancer. *JAMA Netw Open*. 2022;5(3):e221093. doi:10.1001/jamanetworkopen.2022.1093

40. Kato H, Kishiwada M, Hayasaki A, et al. Role of serum carcinoma Embryonic antigen (CEA) level in localized pancreatic adenocarcinoma: CEA level before operation is a significant prognostic indicator in patients with locally advanced pancreatic cancer treated with neoadjuvant therapy followed by surgical resection: a retrospective analysis. *Ann Surg*. 2022;275(5):e698-e707. doi:10.1097/SLA.0000000000004148

41. Nakamura Y, Tanese K, Hirai I, Amagai M, Kawakami Y, Funakoshi T. Serum cytokeratin 19 fragment 21-1 and carcinoembryonic antigen combination assay as a biomarker of tumour progression and treatment response in extramammary Paget disease. *Br J Dermatol*. 2019;181(3):535-543. doi:10.1111/bjd.17789

42. Lupu F, Kinasewitz G, Dormer K. The role of endothelial shear stress on haemodynamics, inflammation, coagulation and glycocalyx during sepsis. *J Cell Mol Med*. 2020;24(21): 12258-12271. doi:10.1111/jcmm.15895

43. Shimoyama Y, Umegaki O, Kadono N, Minami T. Presepsin values predict septic acute kidney injury, acute respiratory distress syndrome, disseminated intravascular coagulation, and shock. *Shock*. 2021;55(4):501-506. doi:10.1097/SHK.0000000000001664

44. Zhou X, Luo G. A meta-analysis of the platelet-lymphocyte ratio: a notable prognostic factor in renal cell carcinoma. *Int J Biol Markers*. 2022;37(2):123-133. doi:10.1177/03936155221081536.

45. Saidak Z, Soudet S, Lottin M, et al. A pan-cancer analysis of the human tumor coagulome and its link to the tumor immune microenvironment. *Cancer Immunol Immunother*. 2021;70(4): 923-933. doi:10.1007/s00262-020-02739-w.

46. Dong Y, Ma WM, Yang W, et al. Identification of C3 and FN1 as potential biomarkers associated with progression and prognosis for clear cell renal cell carcinoma. *BMC Cancer*. 2021;21(1): 1135. doi:10.1186/s12885-021-08818-0

47. Thrumurthy SG, Chaudry MA, Thrumurthy SSD, Mughal M. Oesophageal cancer: risks, prevention, and diagnosis. *BMJ*. 2019;366:l4373. doi:10.1136/bmj.l4373

48. Yaegashi Y, Onoda T, Morioka S, et al. Joint effects of smoking and alcohol drinking on esophageal cancer mortality in Japanese men: findings from the Japan collaborative cohort study. *Asian Pac J Cancer Prev*. 2014;15(2):1023-1029. doi:10.7314/apjcp.2014.15.2.1023